11th World Congress on Computational Mechanics (WCCM XI)
5th European Conference on Computational Mechanics (ECCM V)
6th European Conference on Computational Fluid Dynamics (ECFD VI)
E. Oñate, J. Oliver and A. Huerta (Eds)

MIMETIC LEAST-SQUARES: A LEAST-SQUARES FORMULATION WITH EXACT CONSERVATION PROPERTIES

Pavel Bochev[⋆] and Marc Gerritsma[†]

[*] Sandia National Laboratories, Computational Mathematics and Algorithms, Mail Stop 1110, Albuquerque, NM 87185, USA.
e-mail: pbboche@sandia.gov, Web page: http://www.sandia.gov/ pbboche/

[†]Delft University of Technology, Faculty of Aerospace Engineering, Kluyverweg 2, 2629 HT Delft, The Netherlands
e-mail: M.I.Gerritsma@TUDelft.nl - Web page: http://www.tudelft.nl/

Key words: Least-squares, mimetic methods, conservation, spectral methods.

Abstract. We present a spectral mimetic least-squares method which is fully conservative and decouples the primal and dual variables.

1 INTRODUCTION

We consider the model diffusion-reaction problem

$$\begin{aligned} -\nabla \cdot \mathbb{A}\nabla\phi + \gamma\phi &= f \quad \text{in } \Omega \ , \\ \phi &= g \quad \text{on } \Gamma_D \ , \\ \boldsymbol{n} \cdot \mathbb{A}\nabla\phi &= h \quad \text{on } \Gamma_N \ , \end{aligned} \tag{1}$$

where $\Omega \subset \mathbb{R}^n$ has a Lipschitz-continuous boundary $\partial\Omega = \Gamma_D \cup \Gamma_N$ and $\boldsymbol{n}$ is the outward unit normal to $\partial\Omega$. We assume that $\mathbb{A}$ is a symmetric positive definite tensor and γ is a real-valued, strictly positive function, i.e., there exist constants $f_{min}, f_{max}, \gamma_{min}, \gamma_{max} > 0$ such that

$$f_{min}\boldsymbol{\xi}^T\boldsymbol{\xi} \le \boldsymbol{\xi}^T\mathbb{A}(\mathbf{x})\boldsymbol{\xi} \le f_{max}\boldsymbol{\xi}^T\boldsymbol{\xi} \quad \text{and} \quad \gamma_{min} \le \gamma(\mathbf{x}) \le \gamma_{max} \ , \tag{2}$$

for all $\boldsymbol{x} \in \Omega$ and $\boldsymbol{\xi} \in T_{\mathbf{x}}\Omega$. The tensor $\mathbb{A}$ and the function γ describe material properties. For instance, in heat transfer applications $\mathbb{A}$ is the thermal conductivity of the material and γ can be related to the specific heat capacity.

Almost all published least-squares methods for (1) start with the reformulation of the governing equations into an equivalent first-order system

$$\begin{aligned} \nabla \cdot \boldsymbol{u} + \gamma\phi &= f \quad \text{in } \ \Omega \ , \\ \boldsymbol{u} + \mathbb{A}\nabla\phi &= 0 \quad \text{in } \ \Omega \ , \\ \phi &= g \quad \text{on } \ \Gamma_D \ , \\ \boldsymbol{n} \cdot \boldsymbol{u} &= -h \quad \text{on } \ \Gamma_N \ . \end{aligned} \tag{3}$$

followed by setting up a least-squares functional

$$\mathcal{J}(\boldsymbol{u},\phi;f) := \frac{1}{2}\left(\|\nabla\cdot\boldsymbol{u}+\gamma\phi-f\|_X^2+\|\boldsymbol{u}+\mathbb{A}\nabla\phi\|_Y^2\right)\ , \tag{4}$$

and a least-squares principle, which is the following unconstrained minimization problem:

$$(\boldsymbol{u},\phi) = \arg\min_{\boldsymbol{v}\in U,\,\varphi\in V} \mathcal{J}(\boldsymbol{v},\varphi;f)\ . \tag{5}$$

We will refer to ϕ and $\boldsymbol{u}$ as the *potential* and *flux* variables. In (4)–(5) X, Y and U, V are some appropriate *data* and *solution* spaces. The key juncture in the definition of a well-posed least-squares method is to choose these spaces such that $\mathcal{J}$ is norm-equivalent, i.e., the residual "energy" $|||(\boldsymbol{u},\phi)||| := \mathcal{J}(\boldsymbol{u},\phi;0)$ defines an equivalent norm on the solution spaces:

$$C_1\left(\|\boldsymbol{v}\|_U^2+\|\varphi\|_V^2\right) \le |||(\boldsymbol{v},\varphi)|||^2 \le C_2\left(\|\boldsymbol{v}\|_U^2+\|\varphi\|_V^2\right)\ ,\quad \forall\boldsymbol{v}\in U,\ \varphi\in V\ . \tag{6}$$

One common choice for which (6) holds is $X = Y = L^2(\Omega)$, $U = H(div,\Omega)$ and $V = H^1(\Omega)$. Because strong coercivity is inherited on subspaces, one can approximate both solution spaces by standard C^0 elements. Since the inception of least-squares methods this has often been quoted as one of their principal advantages. However, when formulated in this way, the least-squares method is not conservative [9, 10, 14] and in some cases solutions can be very inaccurate; see [4, 5] for examples.

In this paper we extend these ideas to develop a *spectral* mimetic least-squares method for (1) that is locally conservative. Reformulation of the model problem into a *four-field* first-order system involving two scalar and two vector variables allows us to shift material parameters from the differential operators into a pair of constitutive relations. The four-field system prompts the inclusion of two new equation residuals to the standard least-squares formulation (4). We show that the resulting least-squares principle satisfies exactly the differential equations, while the constitutive relations are satisfied approximately. The key idea then is to approximate the four fields by finite elements from a discrete exact sequence. This allows us to satisfy exactly the differential equations in the discrete setting and yields a locally conservative least-squares method.

2 The model problem deconstructed

Our starting point is the following least-squares principle for the first-order system (3):

$$\min_{\phi\in U,\,\boldsymbol{u}\in V}\mathcal{J}(\phi,\boldsymbol{u}) := \frac{1}{2}\left(\left\|\mathbb{A}^{-1/2}\left(\boldsymbol{u}+\mathbb{A}\nabla\phi\right)\right\|_0^2+\left\|\gamma^{-1/2}\left(\gamma\phi+\nabla\cdot\boldsymbol{u}-f\right)\right\|_0^2\right)\ . \tag{7}$$

To motivate the mimetic least-squares method we reformulate (1) into an equivalent first-order system involving two scalar and two vector variables. To this end, we introduce two more variables defined by

$$\boldsymbol{v} = \mathbb{A}^{-1}\boldsymbol{u} \quad\text{and}\quad \psi = \gamma\phi\ , \tag{8}$$

respectively. Then, the model problem (1) can be written as

$$\begin{array}{llll} \nabla\cdot\boldsymbol{u}+\psi=f \quad \text{in }\Omega\,, & \boldsymbol{v}=\mathbb{A}^{-1}\boldsymbol{u} \quad \text{in }\Omega\,, & \text{and} & \phi=g \quad \text{on }\Gamma_D\,, \\ \boldsymbol{v}+\nabla\phi=0 \quad \text{in }\Omega\,, & \psi=\gamma\phi \quad \text{in }\Omega\,, & & -\boldsymbol{n}\cdot\boldsymbol{u}=h \quad \text{on }\Gamma_N\,. \end{array} \tag{9}$$

As a result of these substitutions, the first two equations

$$\nabla\cdot\boldsymbol{u}+\psi=f \quad \text{and} \quad \boldsymbol{v}+\nabla\phi=0\,, \tag{10}$$

have become independent of the material properties $\mathbb{A}$ and γ. The first equation expresses a conservation law, which can be directly related to the fluxes $\boldsymbol{u}\cdot\boldsymbol{n}$ over the boundary of a volume and the second equation expresses the fact that $\nabla\times\boldsymbol{v}\equiv 0$.

The two new equations, (8), are constitutive laws involving the material parameters. Note that these laws do *not* involve derivatives. By introducing $\boldsymbol{v}$ as a new variable, we have $\boldsymbol{u}$ for the flux and $\boldsymbol{v}$ for the velocity which allows for an independent discrete representation.

The two differential equations, $\nabla\cdot\boldsymbol{u}+\psi=f$ and $\boldsymbol{v}+\nabla\phi=0$, only depend on the space topology and, in the discrete setting, on the grid topology.

Motivated by these properties of mimetic methods we define a new least-squares functional by augmenting (7) with the residuals of the "topological" equations (10)

$$\begin{aligned} &\mathcal{J}((\phi,\boldsymbol{v}),(\psi,\boldsymbol{u});f)= \\ &\frac{1}{2}\left(\left\|\mathbb{A}^{-1/2}(\boldsymbol{u}+\mathbb{A}\nabla\phi)\right\|_0^2+\left\|\gamma^{-1/2}(\gamma\phi+\nabla\cdot\boldsymbol{u}-f)\right\|_0^2+\left\|\boldsymbol{v}+\nabla\phi\right\|_0^2+\left\|\nabla\cdot\boldsymbol{u}+\psi-f\right\|_0^2\right), \end{aligned} \tag{11}$$

and consider the associated least-squares principle

$$\min_{(\phi,\boldsymbol{v})\in U,(\psi,\boldsymbol{u})\in V}\mathcal{J}((\phi,\boldsymbol{v}),(\psi,\boldsymbol{u});f) \tag{12}$$

where $U=H^1(\Omega)\times(L^2(\Omega))^n$ and $V=L^2(\Omega)\times H(div,\Omega)$.

Our first result shows that (12) is a well-posed minimization problem.

Theorem 1. *For homogeneous boundary conditions, $g=h=0$, the least-squares functional $\mathcal{J}((\phi,\boldsymbol{v}),(\psi,\boldsymbol{u});0)$ is norm-equivalent:*

$$\mathcal{J}((\phi,\boldsymbol{v}),(\psi,\boldsymbol{u});0)\sim\|\boldsymbol{u}\|_{H(div,\Omega)}+\|\phi\|_{H^1(\Omega)}+\|\boldsymbol{v}\|_{L^2(\Omega)}+\|\psi\|_{L^2(\Omega)}\,. \tag{13}$$

Proof. Owing to the assumptions (2) it suffices to prove the theorem for $\mathbb{A}=\mathbb{I}$ and $\gamma=1$. Expanding the terms in the least-squares functional yields

$$\begin{aligned} 2\mathcal{J}((\phi,\boldsymbol{v}),(\psi,\boldsymbol{u});0)&=\|\boldsymbol{u}\|_0^2+2\|\nabla\cdot\boldsymbol{u}\|_0^2+2\|\nabla\phi\|_0^2+\|\phi\|_0^2+\|\boldsymbol{v}\|_0^2+\|\psi\|_0^2 \\ &+2(\boldsymbol{u},\nabla\phi)+2(\nabla\cdot\boldsymbol{u},\phi)+2(\boldsymbol{v},\nabla\phi)+2(\nabla\cdot\boldsymbol{u},\psi). \end{aligned} \tag{14}$$

The sum of the first two inner-products vanishes for homogeneous boundary conditions

$$2(\boldsymbol{u}, \nabla\phi) + 2(\nabla \cdot \boldsymbol{u}, \phi) = 2\int_{\partial\Omega} \phi(\boldsymbol{u}\cdot\boldsymbol{n})\,\mathrm{d}S = 0\,.$$

For the remaining two inner products we use the Young's inequality:

$$2(\boldsymbol{v}, \nabla\phi) \geq -\delta\|\boldsymbol{v}\|_0^2 - \frac{1}{\delta}\|\nabla\phi\|_0^2 \quad \text{and} \quad 2(\nabla\cdot\boldsymbol{u}, \psi) \geq -\delta\|\psi\|_0^2 - \frac{1}{\delta}\|\nabla\cdot\boldsymbol{u}\|_0^2\,.$$

Combining with (14) yields

$$2\mathcal{J}((\phi,\boldsymbol{v}),(\psi,\boldsymbol{u});0) \geq \|\boldsymbol{u}\|_0^2 + \left(2-\frac{1}{\delta}\right)\left(\|\nabla\cdot\boldsymbol{u}\|_0^2 + \|\nabla\phi\|_0^2\right) + \|\phi\|_0^2 + (1-\delta)\left(\|\boldsymbol{v}\|_0^2 + \|\psi\|_0^2\right)$$

The theorem follows by choosing any $1/2 < \delta < 1$. □

The next result provides some information about the conservation properties of (12).

Proposition 1. *The minimizers of (11) satisfy (10) in* $L^2(\Omega)$.

Proof. The variations of the least-squares functional in (11) with respect to $\boldsymbol{v}$ and ψ yield the equations

$$\int_\Omega (\boldsymbol{v}+\nabla\phi)\cdot\tilde{\boldsymbol{v}}\,\mathrm{d}x = 0 \;\; \forall\tilde{\boldsymbol{v}}\in L^2(\Omega) \quad \text{and} \quad \int_\Omega (\nabla\cdot\boldsymbol{u}+\psi-f)\tilde{\psi}\,\mathrm{d}x = 0 \;\; \forall\tilde{\psi}\in L^2(\Omega)\,, \qquad (15)$$

respectively. The minimizers of (11) necessarily satisfy these equations, which implies that (10) hold in L^2-sense. □

Proposition 2. *If (10) is satisfied in* $L^2(\Omega)$*, then the equations for* ϕ *and* $\boldsymbol{u}$ *decouple.*

Proof. The variations of the least-squares functional in (11) with respect to $\boldsymbol{u}$ and ϕ yield the equations

$$\int_\Omega \gamma^{-1}\nabla\cdot\boldsymbol{u}\nabla\cdot\tilde{\boldsymbol{u}}\,\mathrm{d}x + \int_\Omega \boldsymbol{u}\mathbb{A}^{-1}\tilde{\boldsymbol{u}}\,\mathrm{d}x - \int_\Omega \gamma^{-1} f\nabla\cdot\tilde{\boldsymbol{u}}\,\mathrm{d}x = \int_\Omega (\nabla\cdot\boldsymbol{u}+\psi-f)\,\nabla\cdot\tilde{\boldsymbol{u}}\,\mathrm{d}x\,,$$

and

$$\int_\Omega \nabla\phi\mathbb{A}\nabla\tilde{\phi}\,\mathrm{d}x + \int_\Omega \gamma\phi\tilde{\phi}\,\mathrm{d}x - \int_\Omega f\tilde{\phi} = \int_\Omega (\boldsymbol{v}+\nabla\phi)\,\nabla\tilde{\phi}\,\mathrm{d}x\,,$$

for all $\tilde{\boldsymbol{u}} \in H(div,\Omega)$ and $\tilde{\phi}\in H^1(\Omega)$, respectively. Proposition 1 shows that the right hand side of these variational statements vanishes and therefore the equations for ϕ and $\boldsymbol{u}$ decouple. See also [4] for a similar decoupling in a constrained formulation. □

2.1 A mimetic least-squares method

Suppose that $U^h = G^h \times C^h$ and $V^h = S^h \times D^h$ are compatible finite element discretizations of U and V such that $\{G^h, C^h\}$ and $\{D^h, S^h\}$ belong in a discrete DeRham complex [1, 6]. In other words, there holds

$$\nabla\phi^h \in C^h \quad \forall \phi^h \in G^h \quad \text{and} \quad \nabla\cdot\boldsymbol{u}^h \in S^h \quad \forall \boldsymbol{u}^h \in D^h . \tag{16}$$

We define the mimetic least-squares principle for (9) as the restriction of (12) to the discrete spaces U^h and V^h:

$$\min_{(\phi^h,\boldsymbol{v}^h)\in U^h,(\psi^h,\boldsymbol{u}^h)\in V^h} \mathcal{J}((\phi^h,\boldsymbol{v}^h),(\psi^h,\boldsymbol{u}^h);f). \tag{17}$$

Because U^h and V^h are conforming spaces, the norm equivalence (13) continues to hold and (17) is a well-posed minimization problem. In addition, the least-squares solution is *locally conservative*.

Theorem 2. *Let* $\{(\phi^h,\boldsymbol{v}^h),(\psi^h,\boldsymbol{u}^h)\} \in U^h \times V^h$ *be a minimizer of (17). Then,*

$$\boldsymbol{v}^h + \nabla\phi^h = 0 \quad \textit{and} \quad \nabla\cdot\boldsymbol{u}^h + \psi^h = P_S f \tag{18}$$

where P_S *is the* L^2 *projection on* S^h*.*

Proof. Consider first the gradient equation in (18). The minimizers of (17) necessarily satisfy the equations

$$\int_\Omega (\boldsymbol{v}^h + \nabla\phi^h)\cdot\tilde{\boldsymbol{v}}^h \,\mathrm{d}x = 0 \;\; \forall \tilde{\boldsymbol{v}}^h \in C^h$$

Since $\nabla\phi^h \in C^h$ there exists $\boldsymbol{v}^h_\phi = -\nabla\phi^h$ and so, the first equation holds for the pair $\{\phi^h, \boldsymbol{v}^h_\phi\}$. By the uniqueness of the least-squares minimizer it follows that $\boldsymbol{v}^h = \boldsymbol{v}^h_\phi$.

Consider now the second equation in (18). The weak equation

$$\int_\Omega (\nabla\cdot\boldsymbol{u}^h + \psi^h - f)\tilde{\psi}^h \,\mathrm{d}x \equiv \int_\Omega (\nabla\cdot\boldsymbol{u}^h + \psi^h - P_S f)\tilde{\psi}^h \,\mathrm{d}x = 0 \;\; \forall\tilde{\psi}^h \in S^h ,$$

is a necessary condition for (17). Since $\nabla\cdot\boldsymbol{u}^h \in S^h$ there exists ψ^h_u such that $\nabla\cdot\boldsymbol{u}^h + \psi^h_u = P_S f$. Again, the uniqueness of the least-squares solution implies that $\psi^h = \psi^h_u$. □

Corollary 1. *Let* $\{(\phi^h,\boldsymbol{v}^h),(\psi^h,\boldsymbol{u}^h)\} \in U^h \times V^h$ *then the discrete equations for* ϕ^h *and* $\boldsymbol{u}^h$ *decouple in the variational formulation.*

Proof. Take variations with respect to ϕ^h and $\boldsymbol{u}^h$ to obtain weak forms similar to the ones in the proof Proposition 2 and use the fact that $U^h \times V^h$ is a conforming subspace of $(H^1(\Omega), L^2(\Omega)) \times (L^2(\Omega), H(div,\Omega))$ which implies that Theorem 2 also holds on the finite dimensional subspace. □

Remark 1. *Note that the results of Theorem 2 and Corollary 1 do not require U^h and V^h to be defined on the same grid. Thus, in principle, one can implement the least-squares method (17) using two different grid partitions of these spaces, i.e., we can consider formulations in which the gradient and divergence equations live on different grids.*

Remark 2. *We started with a scalar diffusion-reaction equation and decomposed it into topological equations and constitutive equations. This adds two vector fields, $\mathbf{v}$ and $\mathbf{u}$ and one scalar field ψ to the system, thus making the system approximately 6 times as large in 2D and 8 times as big in 3D. Due to Proposition 2 and Corollary 1, we can solve all ϕ and $\mathbf{u}$ independently and the solution of $\mathbf{v}$ and ψ can be obtained in a simple post-processing step which avoids the solution of linear systems.*

3 Spectral basis functions

The spectral basis functions used for the mimetic least-squares formulation are the ones initially described in [7, 8, 11] and applied in [12, 13].

3.1 Nodal basis functions

Let $f(\xi)$, $\xi \in [-1,1]$ be smooth function. The reduction of $f(\xi)$ to a 0-cochain on the mesh is given by

$$\mathcal{R}^0(f) = \{f_0, f_1, \ldots, f_N\} \;, \tag{19}$$

where $f_i := f(\xi_i)$ are its nodal values. Consider the Lagrange polynomials $\ell_i^0(\xi)$ given by

$$\ell_i^0(\xi) = \prod_{\substack{j=0 \\ j\neq i}}^{N} \left(\frac{\xi - \xi_j}{\xi_i - \xi_j} \right) \;.$$

We recall that Lagrange polynomials satisfy

$$\ell_i^0(\xi_j) = \begin{cases} 1 & \text{if } i = j \\ 0 & \text{if } i \neq j \end{cases} \qquad \text{and} \qquad \sum_{i=0}^{N} \ell_i^0(\xi) \equiv 1 \;.$$

The corresponding reconstruction of $f(\xi)$ from the 0-cochain $\mathcal{R}^0(f)$ is given by

$$\mathcal{I}^0(f_i)(\xi) = \sum_{i=0}^{N} f_i \ell_i^0(\xi) \quad \Longrightarrow \quad \mathcal{R}^0\left(\mathcal{I}^0(f_i)(\xi)\right) = \sum_{j=0}^{N} f_j \ell_j^0(\xi_i) = f_i \;,$$

and so, $\mathcal{I}^0$ satisfies the consistency property, $\mathcal{R}^0 \circ \mathcal{I}^0 = \mathbb{I}$. For suitably chosen nodes ξ_i and sufficiently smooth $f(\xi)$ one can show that $\mathcal{I}^0 \circ \mathcal{R}^0 = \mathbb{I} + \mathcal{O}(h^p)$. Figure 1 illustrates this property.

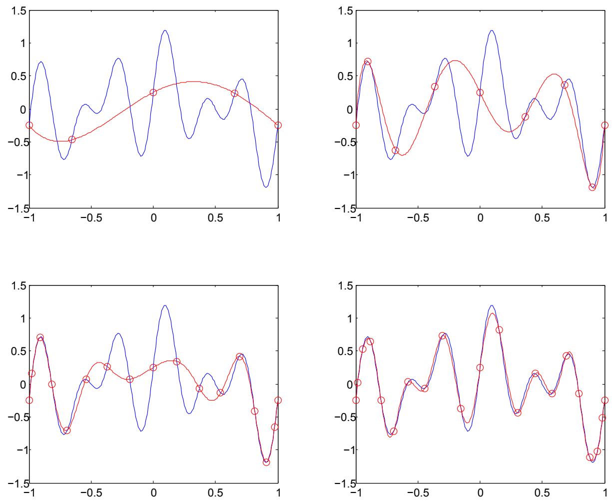

Figure 1: Nodal approximation (red curve) of $f(\xi) = \cos\pi\xi(\sin 5\pi\xi + 0.25)$, (blue curve) for $N = 4, 8, 16, 20$.

3.2 Edge basis functions

We consider again a smooth function $f(\xi)$ but reduce it to a 1-cochain given by

$$\mathcal{R}^1(f) = \{f_1, \ldots, f_N\} \quad \text{where} \quad f_i = \int_{\xi_{i-1}}^{\xi_i} f(\xi)\;, \quad i = 1, \ldots, N\;. \tag{20}$$

Define the edge Lagrangian basis, $\ell_i^1(\xi)$ by [7, 11]

$$\ell_i^1(\xi) = -\frac{d}{d\xi}\sum_{k=0}^{i-1} \ell_k^0(\xi), \quad i = 1, \ldots, N\;. \tag{21}$$

The edge basis functions have the property that

$$\int_{\xi_{j-1}}^{\xi_j} \ell_i^1 = \begin{cases} 1 & \text{if } i = j \\ 0 & \text{if } i \neq j \end{cases}\;, \quad i, j = 1, \ldots, N\;. \tag{22}$$

The reconstruction of $f(\xi)$ from the 1-cochain $\mathcal{R}^1(f)$ is given by

$$\mathcal{I}^1(f_i)(\xi) = \sum_{i=1}^{N} f_i \ell_i^1(\xi) \quad \Longrightarrow \quad \mathcal{R}^1\left(\mathcal{I}^1(f_i)(\xi)\right) = \sum_{i=1}^{N} f_i \int_{\xi_{j-1}}^{\xi_j} \ell_i^1 \overset{(22)}{=} f_j\;, \tag{23}$$

which shows that consistency property, $\mathcal{R}^1 \circ \mathcal{I}^1 = \mathbb{I}$, is satisfied. Figure 2 shows that for increasing N the accuracy of the reconstruction improves, $\mathcal{I}^1 \circ \mathcal{R}^1 = \mathbb{I} + O(h^p)$. Figures 1–2 also clearly demonstrate the difference between $\mathcal{I}^0$, which matches the *nodal values* of a function and $\mathcal{I}^1$

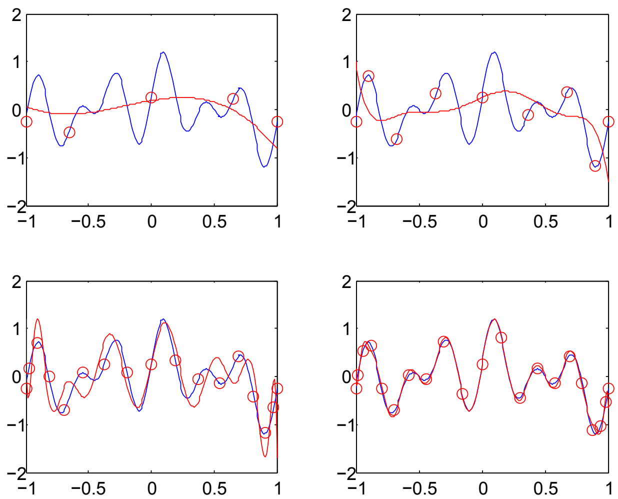

Figure 2: Edge basis approximation (red curve) of $f(x) = \cos\pi\xi(\sin 5\pi\xi + 0.25)$ (blue curve), for $N = 4, 8, 16, 20$.

which matches the *edge integrals* of a function. In particular, $\mathcal{I}^1(f_i)(\xi)$ does not pass through the nodal values f_i, shown by red circles in the figure, i.e., this reconstruction is not nodal.

With these polynomial representations it can be shown that $\delta\mathcal{R}^0 = \mathcal{R}^1\frac{d}{d\xi}$ and $\frac{d}{d\xi}\mathcal{I}^0 = \mathcal{I}^1\delta$, where δ is the coboundary operator which converts in this one dimensional case 0-cochains to 1-cochains, [3]

4 Discretization of the constitutive relations

Discretization of the constitutive laws

$$\boldsymbol{u} = \mathbb{A}\boldsymbol{v} \quad \text{and} \quad \psi = \gamma\phi \,. \tag{24}$$

presents an entirely different situation. Suppose for simplicity that $\mathbb{A} = \mathbb{I}$, $\gamma = 1$ and as before, ϕ, $\boldsymbol{v}$, $\boldsymbol{u}$, and ψ are approximated by 0,1,2 and 3-cochains, respectively. Then, in order for (24) to hold exactly we must have

$$\mathcal{I}^2(\boldsymbol{u}) = \mathcal{I}^1(\boldsymbol{v}) \quad \text{and} \quad \mathcal{I}^3(\psi) = \mathcal{I}^0(\phi) \,. \tag{25}$$

However, it is easy to see that relationships such as (25) may not even hold true if the *same* function is reduced to different cochains and then reconstructed back, because reconstruction is only an approximate left inverse of the reduction. As a result, in general

$$\mathcal{I}^k \circ \mathcal{R}^k(f) \neq \mathcal{I}^{(n-k)} \circ \mathcal{R}^{(n-k)}(f) \,.$$

Approximation of the smooth function $f(x) = \cos\pi\xi(\sin 5\pi\xi + 0.25)$ by node and edge basis functions in Sections 3.1–3.2 provides a simple illustration of this fact. The reconstruction from

0-cochains $\mathcal{I}^0 \circ \mathcal{R}^0(f)$ is the Lagrange nodal interpolant of $f(x)$, i.e., a polynomial that has the same nodal values on the mesh as $f(x)$. On the other hand, the reconstruction of the same function from 1-cochains, $\mathcal{I}^1 \circ \mathcal{R}^1(f)$, matches the integral of $f(x)$ on every element but not its nodal values, i.e., $\mathcal{I}^1 \circ \mathcal{R}^1(f) \neq \mathcal{I}^0 \circ \mathcal{R}^0(f)$. Figures 1 and 2 clearly show this distinction.

5 Results

In this section we want to illustrate the spectral mimetic least-squares method by means of a test problem. We consider the problem with $\mathbb{A} = \mathbb{I}$ and $\gamma = 1$,

$$-\nabla \cdot \nabla \phi + \phi = f \text{ with } f(x,y) = (2\pi^2+1)\sin(\pi x)\sin(\pi y) \quad \text{and} \quad \phi = 0 \text{ along } \partial\Omega\,,$$

on the domain $\Omega = [-1,1]^2$ with exact solution $\phi_{ex}(x,t) = \sin(\pi x)\sin(\pi y)$.

The domain is divided in $K \times K$ elements. The solution is represented on the reference domain $(\xi,\eta) \in \Omega_{ref} = [-1,1]^2$ and mapped onto the respective elements in (x,y)-coordinates. We will use the following polynomial expansions for ϕ, ψ, $\boldsymbol{v}$ and $\boldsymbol{u}$

$$\phi^h(\xi,\eta) = \sum_{i=0}^{N}\sum_{j=0}^{N} \phi_{i,j}\ell_i^0(\xi)\ell_j^0(\eta) \in \mathbb{P}^{N,N}\,,$$

$$\boldsymbol{v}^h(\xi,\eta) = \sum_{i=1}^{N}\sum_{j=0}^{N} u_{i,j}\ell_i^1(\xi)\ell_j^0(\eta) + \sum_{i=0}^{N}\sum_{j=1}^{N} v_{i,j}\ell_i^0(\xi)\ell_j^1(\eta) \in \mathbb{P}^{N-1,N} \times \mathbb{P}^{N,N-1}\,,$$

$$\boldsymbol{u}^h(\xi,\eta) = \sum_{i=0}^{\tilde{N}}\sum_{j=1}^{\tilde{N}} p_{i,j}\tilde{\ell}_i^0(\xi)\tilde{\ell}_j^1(\eta) - \sum_{i=1}^{\tilde{N}}\sum_{j=0}^{\tilde{N}} q_{i,j}\tilde{\ell}_i^1(\xi)\tilde{\ell}_j^0(\eta) \in \mathbb{P}^{\tilde{N},\tilde{N}-1} \times \mathbb{P}^{\tilde{N}-1,\tilde{N}}\,,$$

$$\psi^h(\xi,\eta) = \sum_{i=1}^{\tilde{N}}\sum_{j=1}^{\tilde{N}} \psi_{i,j}\tilde{\ell}_i^1(\xi)\tilde{\ell}_j^1(\eta) \in \mathbb{P}^{\tilde{N}-1,\tilde{N}-1}\,,$$

where N denotes the polynomial degree on the primal grid and $\tilde{N}$ denotes the polynomial degree on the dual grid. Due to the decoupling at the continous level, Proposition 2, and at the discrete level, Corollary 1, N and $\tilde{N}$ can be chosen independently. These polynomial spaces are compatible with the gradient on the primal grid and the divergence on the dual grid, see also [6]. With this polynomial reconstruction of the cochains, ϕ^h is globally C^0, $\boldsymbol{v}^h$ has tangential continuity between elements, $\boldsymbol{u}^h$ has normal continuity and ψ^h is discontinuous between elements.

5.1 Different polynomial representations on dual elements

In Remarks 1 it was pointed out that for a mimetic least-squares formulation it is *not* necessary to have a strict one-to-one relation between dual variables. In this section we will show that we can use different polynomial degrees on dual elements. In Figures 3, 4 and 5 results are presented for the case $N = \tilde{N} + 1$, which violates strict duality. The conservation laws are still satisfied up to machine precision as shown in Figure 5, which was to be expected since the conservation laws are represented on one mesh only and are completely insensitive to the representation of the dual variables.

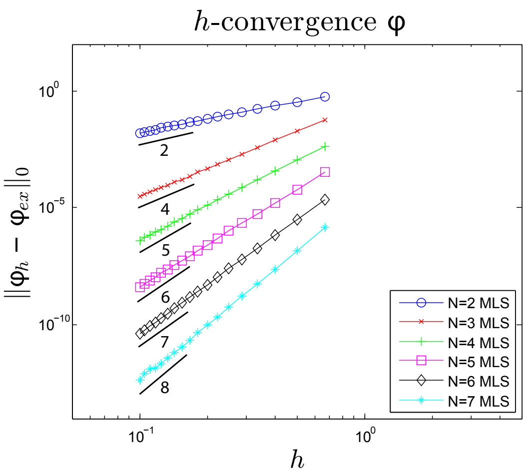

(a) h-convergence ϕ

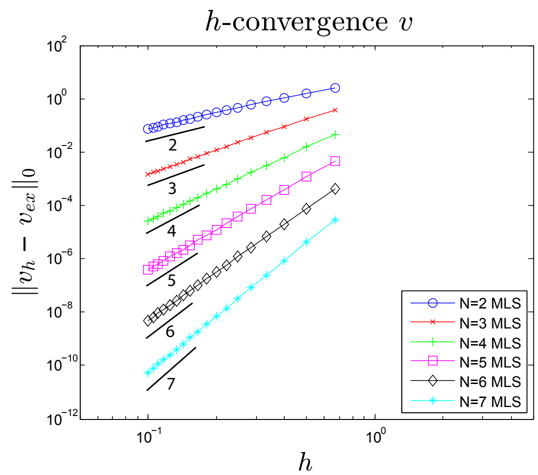

(b) h-convergence v

Figure 3: h-convergence for ϕ and $\boldsymbol{v}$ for various polynomial orders on a uniform orthogonal grid for the mimetic least-squares functional for the case $N = \tilde{N} + 1$. The observed rate of convergence is indicated by the black slope lines.

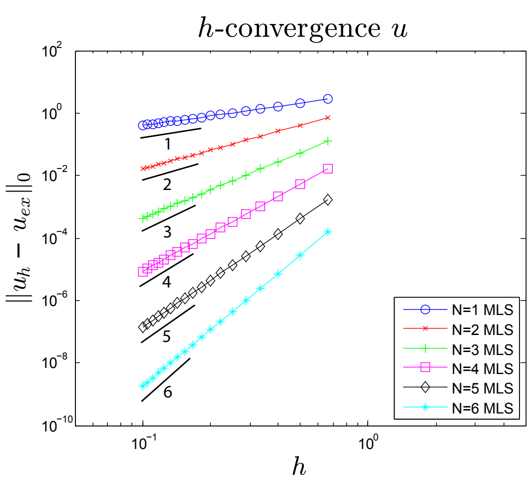

(a) h-convergence u

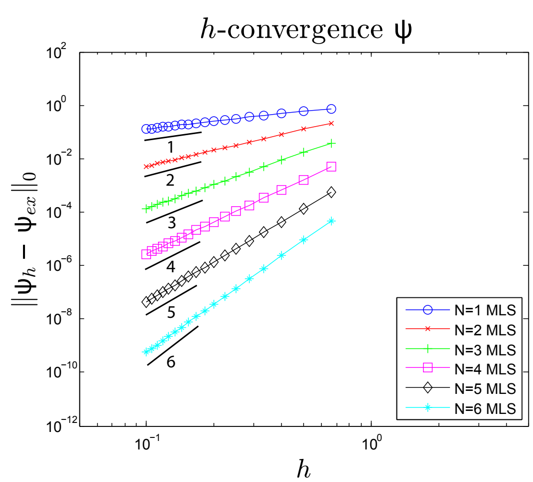

(b) h-convergence ψ

Figure 4: h-convergence for $\boldsymbol{u}$ and ψ for various polynomial orders on a uniform orthogonal grid for the mimetic least-squares functional for the case $N = \tilde{N} + 1$. The observed rate of convergence is indicated by the black slope lines.

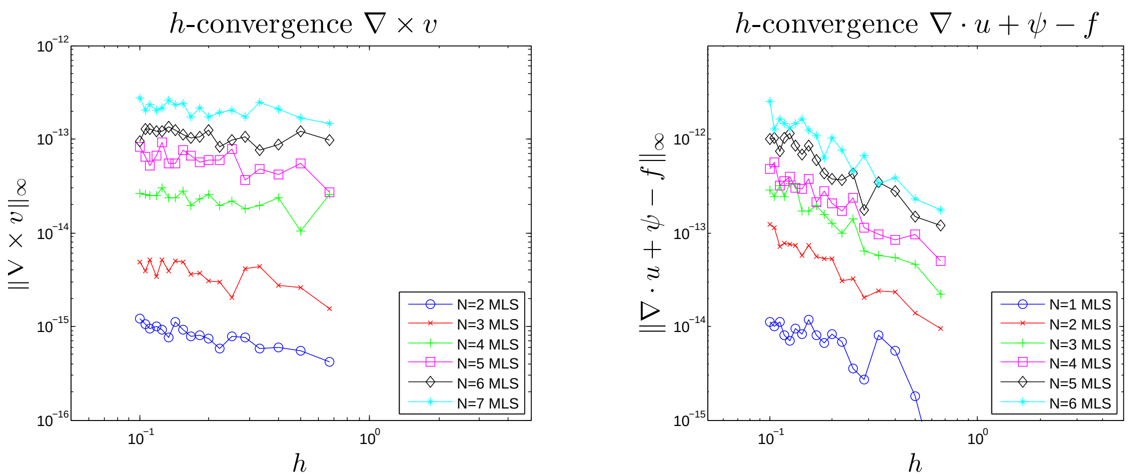

(a) h-convergence u (b) h-convergence ψ

Figure 5: h-convergence for $\nabla \times \boldsymbol{v}$ and $\nabla \cdot \boldsymbol{u} + \psi - f$ for various polynomial orders on a uniform orthogonal grid for the mimetic least-squares functional for the case $N = \tilde{N} + 1$.

6 Conclusions

In this paper a spectral mimetic least-squares formulation is presented for reaction-diffusion problems. Topological operations like the gradient, curl and divergence can be satisfied up to machine precision in this formulation. We conclude that two requirements are necessary for a mimetic least-squares formulation:

1. The discrete space should allow for a discrete representation for the topological operators, see Section 3;

2. The least-squares functional should decouple the topological relations from the metric-dependent relations.

The mimetic least-squares method still leads to a positive definite system. We do not need to satisfy an inf-sup condition. The use of standard C^0-elements needs to be abandoned in favor of basis functions which preserve the geometric degrees of freedom. These conclusions are confirmed by numerical results presented in Section 5. A more extensive description of this method and the application to non-affine grids can be found in [3].

References

[1] Arnold, D.N. and Falk, R.S. and Winther, R., Finite element exterior calculus: from Hodge theory to numerical stability, *American mathematical society*, (2010), **47**, 281–354.

[2] Bochev, P. and Hyman, J., *Principles of mimetic disrcertizations of differential operators*, in Compatible Spatial Discretizations, Eds. D. Arnold, P. Bochev, R. Nicolaides and M.

Shashkov, The IMA volumes in Mathematics and its Applications, Springer Verlag, 89-119, 2006.

[3] Bochev, P.B. and Gerritsma, M.I., A spectral Mimetic Least-Squares Method, submitted to *Computers & Mathematics with Applications*, 2014.

[4] Bochev, P. and Gunzburger, M., A locally conservative least-squares method fot Darcy flows, *Commun. Numer. Meth. Engng.*, (2008), **24**, 97-110.

[5] Chang, C. and Nelson, J., Least-squares finite element method for the Stokes problem with zero residual of mass conservation, *SIAM Journal of Numerical Analysis*, (1997), **34**, 480-489.

[6] Demkowicz, L., *Polynomial Exact Sequences and Projection-Based Interpolation with Application to Maxwell Equations*, in Mixed Finite Elements, Compatibility Conditions, and Applications, Springer, 2008.

[7] Gerritsma, M.I., *Edge functions for spectral element methods* in Spectral and High Order Methods for Partial Differential Equations, Springer Lecture Notes in Computational Science and Engineering, 199-208, (2011).

[8] Gerritsma, M.I., An introduction to a compatible spectral discretization method, *Mechanics of Advanced Materials and Structures*, (2012), **19**, 48-67.

[9] Heys, J.J. and Lee, E. and Manteuffel, T.A. and McCormick, S.F., On mass-conserving least-squares methods, *SIAM Journal on Scientific Computing*, (2006), **28**, 1675-1693.

[10] Heys, J.J. and Lee, E. and Manteuffel, T.A. and McCormick, S.F., An alternative least-squares formulation of the Navier-Stokes equations with improved mass conservation, *Journal of Computational Physics*, (2007), **226**, 994-1006.

[11] Kreeft, J. and Palha, A. and Gerritsma, M., Mimetic framework on curvilinear quadrilaterals of arbitrary order, *arXiv:1111.4304*, (2011).

[12] Kreeft, J. and Gerritsma, M., Mixed mimetic spectral element method for Stokes flow: A pointwise divergence-free solution, *Journal of Computational Physics*, (2013), **240**, 284-309.

[13] Palha, A., Rebelo, P., Hiemstra, R., Kreeft, J. and Gerritsma, M.I., Physics-compatible discretization techniques on single and dual grids, with application to the Poisson equation for volume forms, *Journal of Computational Physics*, (2014), **257**, 1394-1422.

[14] Proot, M.M.J. and Gerritsma, M.I., Mass- and momentum conservation of the least-squares spectral element method for the Stokes problem, *Journal of Scientific Computing*, (2006), **27**, 389-401.